

Supplementary Material-

Initiation of RAFT Polymerization: Electrochemically Initiated RAFT Polymerization in Emulsion (Emulsion eRAFT), and Direct PhotoRAFT Polymerization of Liquid Crystalline Monomers

Caroline Bray,^{A,B} Guoxin Li,^A Almar Postma,^A Lisa T. Strover,^{A,B} Jade Wang,^A and Graeme Moad^{A,B}

^ACSIRO Manufacturing, Clayton, Vic. 3168, Australia.

^BCorresponding authors. Email: caroline.bray@csiro.au; lisa.strover@csiro.au; graeme.moad@csiro.au

Part 1. Electrochemically-Initiated RAFT Polymerization in Emulsion (Emulsion eRAFT).

Materials

Monomers (*n*-butyl acrylate (BA; $\geq 99\%$, inhibited with 10-60 ppm MEHQ)), styrene (St; ReagentPlus, $\geq 99\%$, with 4-*tert*-butyl catchetol as stabilizer), and *N,N*-dimethylacrylamide (DMAm; 99% , inhibited with 500 ppm MEHQ)), were purchased from Sigma-Aldrich and filtered through alumina to remove inhibitor prior to polymerization. Ammonium persulfate (APS; Sigma-Aldrich ACS reagent, $\geq 98\%$) and iron (III) sulfate hydrate ($\text{Fe}_2(\text{SO}_4)_3 \cdot x\text{H}_2\text{O}$; Sigma-Aldrich, 97%), ethylenediaminetetraacetic acid (EDTA; Sigma-Aldrich, 99.995%), potassium chloride (KCl; Merck, 99.5%), and α,α' -azobisisobutyronitrile (AIBN; Acros Organics, 98%) were purchased from commercial suppliers and used as received. Cyanomethyl dodecyl trithiocarbonate (**1**) was prepared as described elsewhere.^[1]

Block copolymer macroRAFT agent synthesis

RAFT-terminated PDMAm was synthesised by thermally initiated RAFT polymerization. DMAm (5.7 mL), cyanomethyl dodecyl trithiocarbonate (**1**, 635 mg), and AIBN (13 mg) were dissolved in 10.8 mL acetonitrile. The solution was purged with nitrogen and polymerization was conducted at $75\text{ }^\circ\text{C}$ for 30 min (**2a** precursor) or $60\text{ }^\circ\text{C}$ for 90 min (**2b** precursor). The polymer was collected by precipitation and dried to obtain the products with (**2a** precursor) M_n (NMR) = 3.2 kDa, M_n (GPC) = 4.3k (PMMA equivalents), and $\mathcal{D} = 1.06$, and (**2b** precursor) M_n (NMR) = 2.1 kDa, M_n (GPC) = 3.5k (PMMA equivalents), and $\mathcal{D} = 1.12$. M_n (NMR) based on monomer conversion as determined by ^1H NMR spectroscopy. The PDMAm macroRAFT agent was dissolved in 10.8 mL acetonitrile with BA (3 mL) and AIBN (13 mg); the solution was purged with nitrogen and polymerization was conducted at $60\text{ }^\circ\text{C}$ for 165 min (**2a**) or 187 min (**2b**). The block copolymer compositions were obtained by precipitation and dried, with (**2a**) M_n (NMR) = 4.2 kDa, M_n (GPC) = 4.9k (PMMA equivalents), and $\mathcal{D} = 1.08$, and (**2b**) M_n (NMR) = 3.1 kDa, M_n (GPC) = 5.3k (PMMA equivalents), and $\mathcal{D} = 1.09$. The ^1H NMR spectra (**Figure S1**) showed the block copolymers to be a mixture of the PDMAm macroRAFT agent and PPMAm-*b*-PBA in the ratio 0.15:0.85 (**2a**) or 0.4:0.6 (**2b**). Refer SI part 3 for further analysis details.

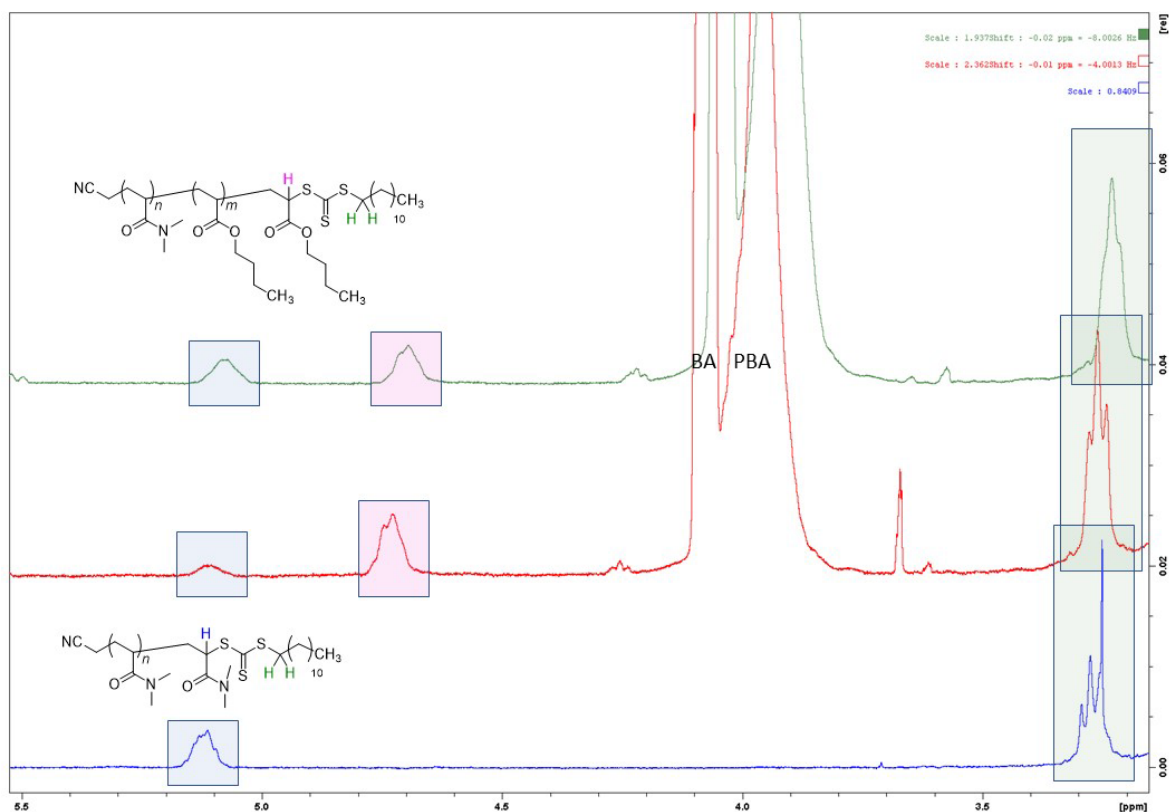


Figure S1. Region of ^1H NMR spectra (CDCl_3) of PDMAm macroRAFT agent (bottom) and PDMAm-*b*-PBA **2a** (middle) and **2b** (top).

*e*RAFT emulsion polymerization

*e*RAFT emulsion polymerisations were conducted in a 3-electrode bulk electrolysis cell with a GC rod counter electrode, GC rod working electrode, and an Ag/AgCl reference electrode. Experiments were controlled and monitored with an Autolab PGSTAT 302N potentiostat. PDMAm-*b*-PBA, styrene, iron(III) sulfate, EDTA, and APS were added to the cell in a 406:1:0.2:0.2:0.2 ratio (EM1 using BCP **2a**); 406:1:0.2:0.2:0 ratio (EM2 using BCP **2b**), with 0.2 equiv. APS added after 3hr; or 442:1:0.1:0.1:0.1 ratio (EM3 using BCP **2b**) - with St:BCP ratios based on BCP M_n as determined by GPC - along with water to make up a 27 % (v/v) mixture with respect to styrene, and 0.1 M KCl supporting electrolyte. An emulsion was formed by stirring at approx. 250 rpm for 20 min., while purging the cell with nitrogen. Polymerization was initiated by applying a constant potential equal to the reduction potential of the Fe-EDTA species as determined by CV.

The progress of the polymerizations was monitored by NMR spectroscopy and by DLS. The NMR results proved inconclusive due to sample handling difficulties. The DLS data are reported in Figure S2 and show that for the conditions used, the systems quickly move to a monomodal particle size distribution with Z_{av} diameter in the range 90-120 nm, PDI ~ 0.2.

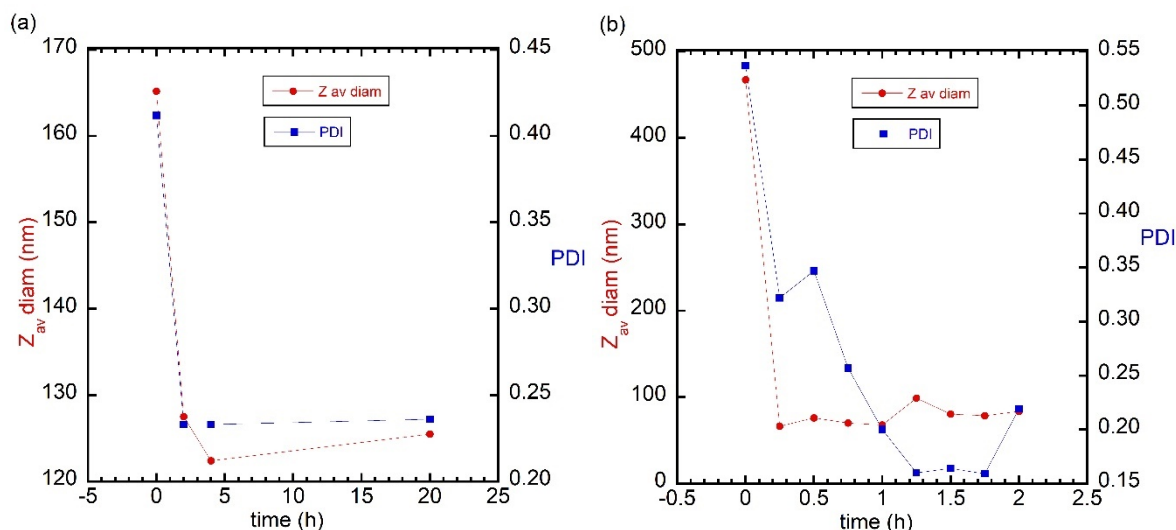


Figure S2. DLS data vs polymerization time for polymerization (a) EM1 and (b) EM3 (refer Table 1 for details of polymerizations).

Characterization

NMR experiments were performed on Bruker Avance 400 MHz NMR spectrometers. NMR experiments were performed with the sample held at 25 ± 0.1 °C for routine analysis. Chemical shifts for all experiments are referenced using the Unified Scale relative to 0.3 % tetramethylsilane in chloroform-*d* (CDCl_3). Samples for NMR spectroscopy were prepared by dissolving the analyte in CDCl_3 and placing the solution into a 5 mm NMR tube. The data were processed using Bruker TopSpin v3.5.7 software.

Gel permeation chromatography (GPC) was performed on a Shimadzu system equipped with a CMB-20A controller system, an SIL-20A HT autosampler, an LC-20AT tandem pump system, a DGU-20A degasser unit, a CTO-20AC column oven, an RDI-10A refractive index detector, and $4 \times$ Waters Styragel columns (HT2, HT3, HT4, and HT5, each $300 \text{ mm} \times 7.8 \text{ mm}$, providing an effective molar mass range of $100 - 4 \times 10^6 \text{ g mol}^{-1}$). *N,N*-Dimethylacetamide (DMAc) containing 4.34 g L^{-1} lithium bromide (LiBr) was used as an eluent with a flow rate of 1 mL/min at 80 °C. Number (M_n) and weight average (M_w) molar masses were evaluated using Shimadzu LC Solution software. The GPC columns were calibrated with low dispersity polystyrene (PSt) standards or poly(methyl methacrylate) (PMMA) standards and molar masses are reported as PMMA (for macroRAFT synthesis) or PSt (for emulsion eRAFT) equivalents. A 3rd-order polynomial was used to fit the $\log M_p$ vs time calibration curve, which was near linear across the relevant molar mass range.

Cyclic voltammetry

CVs were conducted with an Autolab PGSTAT 302N potentiostat, in a nitrogen-purged divided H-cell with a glassy carbon rod counter electrode, 1 mm GC disk working electrode, and Ag/AgCl reference electrode. The working electrode was polished with $0.5 \mu\text{M}$ alumina slurry and thoroughly rinsed before each CV experiment. CVs were conducted in aqueous solution with 0.1 M KCl as supporting electrolyte.

Dynamic Light Scattering (DLS)

Dynamic light scattering measurements were performed on a Malvern Instruments Zetasizer Nano instrument ZEN3600 illuminated with a 4 mW 633 nm HeNe gas laser. An Avalanche photodiode detector measures the back scattered light at a position 173° relative to the angle of the incident light beam. Particle size and distribution was calculated using the Malvern Software, where 20 cumulative measurements were made for each sample and three repeats performed. Measurement were performed on sample of latex diluted 5 drops into 1 mL of MilliQ[®] water. The analyses were performed at 25 °C.



Figure S3. Diluted latex samples for experiment EM3.

Part 2a. High Throughput Synthesis of PDMAm and PDMAm-*b*-PBA macroRAFT Agents.

Materials

N,N-Dimethylacrylamide (DMAm) and butyl acrylate (BA) were purchased from Aldrich and purified by passage through basic alumina. AIBN was re-crystallisation from methanol. The RAFT agent – cyanomethyl dodecyl trithiocarbonate (**1**) was prepared as described elsewhere.^[1] Acetonitrile (dried) was purchased from Merck and used as received.

High throughput Synthesis.

High throughput synthesis was conducted using a ChemSpeed[®] robotic synthesis platform that comprised an iSynth reactor equipped with an array of 12 disposable glass reactor vials each with a capacity of 100 mL.

The following stock solutions were prepared and placed in the reservoir vials.

Stock solution A: DMAm (200 mL) only.

Stock solution B: 1.55 g AIBN in 50 mL acetonitrile.

Stock solution C: 39.572 g RAFT agent **1** in 446.6 mL acetonitrile.

Stock solution D: BA (100 mL) only

All stock solutions were degassed by sparging with nitrogen for 0.5 h.

The reagent reservoirs were loaded in the iSynth reactor deck.

The robotic platform contained 4 individual syringe pumps which enabled multiple reagent solutions to be added simultaneously. Each syringe pump could also be operated individually to deliver different volumes, and at different rates to the other syringes.

The appropriate amounts of the reagent solutions were dispensed from the reservoir vials using the 4-Needle Head tool equipped with two 10 mL and two 1 mL syringes into the separate reactor 100 mL vials within the iSynth[®] reactor, such that there were 12 vials containing monomer, raft agent and initiator solutions. The rate of aspiration and dispensing of the reagent solutions was 10 mL/minute and 20 mL/minute, respectively.

Stock solution A (DMAm alone), stock solution B (AIBN in acetonitrile) and stock solution C (**1** in acetonitrile) were injected into the reactor vials under nitrogen. The polymerizations were carried out at 60 °C for 16 h with vortexing at 400 rpm. On completion, 200 µL of solution was taken from each reactor for NMR analysis.

The requisite amount of stock solution D (BA alone) was injected into reactors and the polymerization was then continued at 60 °C for further 18 h again with vortexing at 400 rpm.

The final reaction solutions were characterized through NMR and GPC analyses. The individual polymerization conditions are summarized in **Table S1**

Table S1. Polymerization conditions for RAFT synthesis of PDMAm and PDMAm-*block*-PBA.

Reactor	First block (60°C/16hrs)			Second block (60°C/18hrs)	
	Stock solution A (mL)	Stock solution B (mL)	Stock solution C (mL)	Stock solution B (mL)	Stock solution D (mL)
1	20.800	1.000	37.360		
2	20.800	1.000	37.360	1.450	2.940
3	20.800	1.000	37.360	1.450	7.350
4	20.800	1.000	37.360	1.450	14.690
5	10.400	2.000	37.360		
6	10.400	2.000	37.360	0.900	2.940
7	10.400	2.000	37.360	0.900	7.350
8	10.400	2.000	37.360	0.900	14.690
9	5.200	3.610	37.360		
10	5.200	3.610	37.360	0	2.940
11	5.200	3.610	37.360	0	7.350
12	5.200	3.610	37.360	0	14.690

Characterization of PDMAm and PDMAm-block-PBA

All homopolymers (PDMAm) and block polymers were characterized by ^1H NMR (CDCl_3 Av400H) and GPC (THF, Waters 2695 GPC system). The results are summarized in Table S2 and Table S3. Selected ^1H NMR (Figure S4) and GPC traces (Figure S6-Figure S9) are shown below. The values M_n (NMR) are based on determination of the residual monomer and calculated using the relationship $[\text{monomer}]_{\text{consumed}}/([\text{RAFT}]) \times M_{\text{monomer}} + M_{\text{RAFT}}$.

Table S2. ^1H NMR and GPC data for PDMAm homopolymers (1st block).

Reactor	Code	Monomer 1	Conversion (%)	DP (DMAm)	M_n (NMR)	M_n (GPC) ^a	\bar{D}
1	DMA20-1	DMAm	97	20.40	2340	2750	1.04
2	DMA20-2	DMAm	98	20.40	2340	2770	1.04
3	DMA20-3	DMAm	98	20.40	2340	2770	1.04
4	DMA20-4	DMAm	97	20.50	2350	2770	1.04
5	DMA10-1	DMAm	98	10.40	1350	1850	1.03
6	DMA10-2	DMAm	98	10.40	1350	1840	1.03
7	DMA10-3	DMAm	98	10.20	1330	1830	1.03
8	DMA10-4	DMAm	97	10.10	1320	1830	1.03
9	DMA5-1	DMAm	95	5.10	820	1440	1.02
10	DMA5-2	DMAm	96	5.20	830	1430	1.01
11	DMA5-3	DMAm	96	5.30	840	1440	1.02
12	DMA5-4	DMAm	96	5.20	830	1440	1.01

^a The GPC traces for the DMA5 and DMA10 series were truncated at the salt peak resulting in an artificially high value for M_n (GPC) and a low value for \bar{D} (Figure S6-Figure S9). Values thought to be affected are shown in red.

Table S3. ^1H NMR and GPC data for the PDMAm-*b*-PBA block copolymers.

Reactor	Code	Monomer 2	conversion (%)	DMAm/BA (mole ratio)	M_n (NMR)	M_n (GPC) ^a	\bar{D}
2	DMA20-BA2	BA	97.29	20.69/2.86	2710	3000	1.04
3	DMA20-BA5	BA	96.93	20.47/5.25	3020	3240	1.05
4	DMA20-BA10	BA	96.12	20.54/10.49	3690	3660	1.05
6	DMA10-BA2	BA	92.23	10.62/2.04	1630	2010	1.04
7	DMA10-BA5	BA	94.64	10.68/5.32	2060	2240	1.05
8	DMA10-BA10	BA	96.06	10.52/10.86	2750	2650	1.06
10	DMA5-BA2	BA	91.56	5.36/2.03	1110	1590	1.03
11	DMA5-BA5	BA	94.36	5.27/5.24	1510	1810	1.04
12	DMA5-BA10	BA	96.17	5.12/10.52	2170	2180	1.05

^a The GPC traces for DMA5 series were truncated at the salt peak resulting in an artificially high M_n (GPC) and a low value for \bar{D} (Figure S6-Figure S9). Values thought to be affected are shown in red.

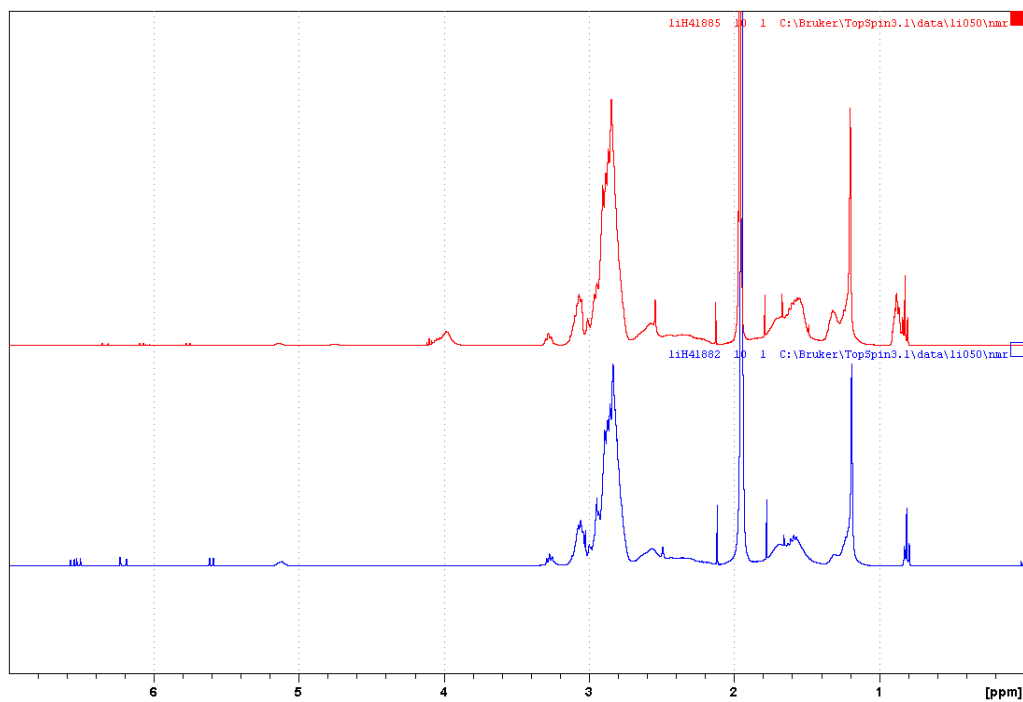


Figure S4. ¹H NMR spectra (400 MHz, CDCl₃) of the final polymerization mixtures for samples DMA20-2 (bottom) and DMA20-BA2 (top).

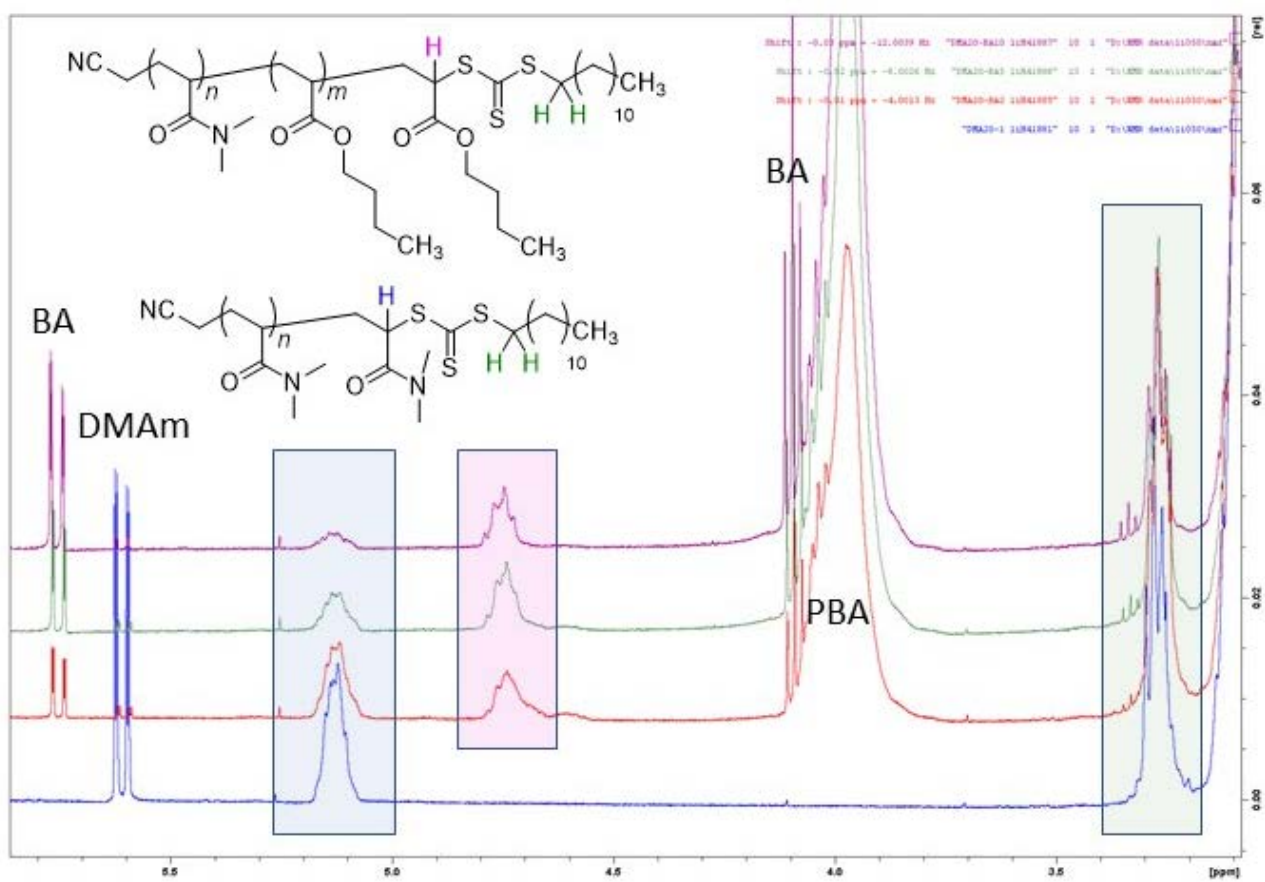


Figure S5. Region of ^1H NMR spectra (400 MHz, CDCl_3) of the final polymerization mixtures for samples DMA20-2, DMA20-BA2, DMA20-BA5, and DMA20-BA10.

The fractions of PDMAm macro RAFT and the desired PDMAm-*b*-BA macro RAFT (Table S4) were determined by integration of the peaks associated with the methine hydrogens α to the trithiocarbonate in the ^1H NMR spectra (e.g., Figure S5). The low yield of block copolymer particularly for short BA blocks can be attributed to the low transfer constant of the PDMAm macroRAFT agent in BA polymerization. Similar conversions of the macroRAFT agent to block copolymer indicate that the transfer constant of the macroRAFT agent does not depend strongly on the molar mass of the PDMAm macroRAFT agent for DP 5-20.

Table S4. Fractions of PDMAm macro RAFT and the desired PDMAm-*b*-BA macro RAFT in various samples.

Sample	Fraction PDMAm macro RAFT	Fraction PDMAm- <i>b</i> -BA macro RAFT
DMA20-BA2	0.66	0.34
DMA20-BA5	0.28	0.72
DMA20-BA10	0.12	0.88
DMA10-BA2	0.65	0.35
DMA10-BA5	0.30	0.70
DMA10-BA10	0.12	0.88
DMA5-BA2	0.62	0.38
DMA5-BA5	0.38	0.62
DMA5-BA10	0.27	0.73

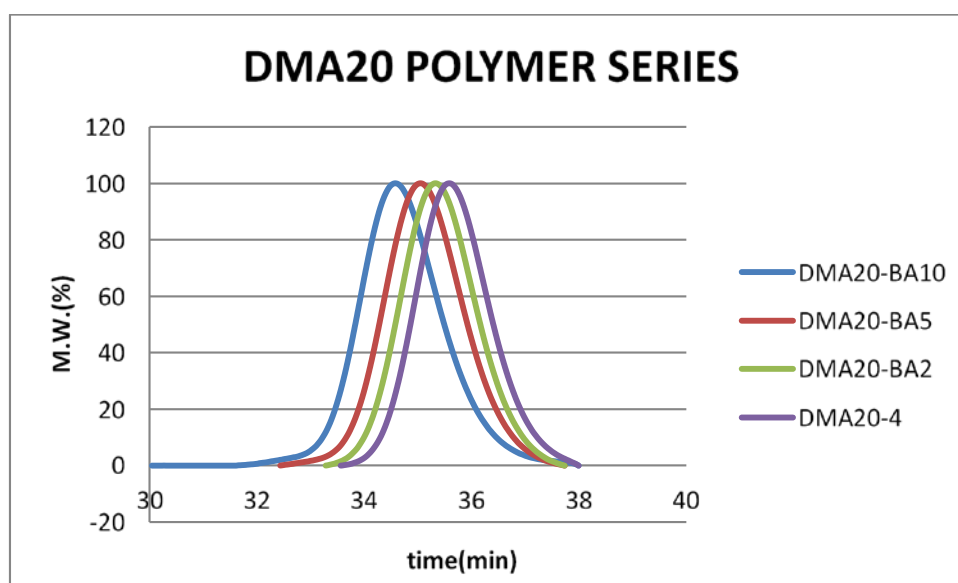


Figure S6. GPC traces of DMA20 series of homopolymer and block polymers

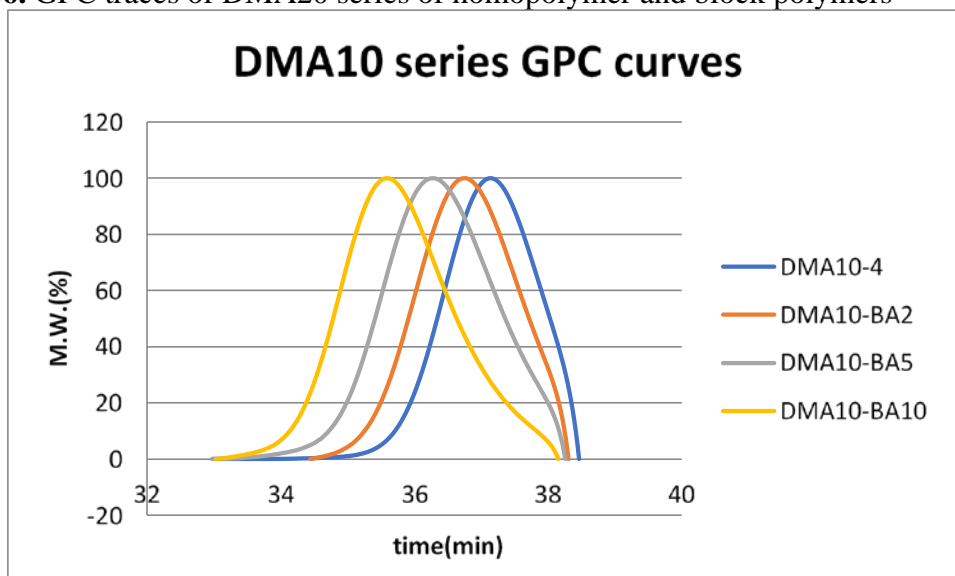


Figure S7. GPC traces of DMA10 series of homopolymer and block polymers

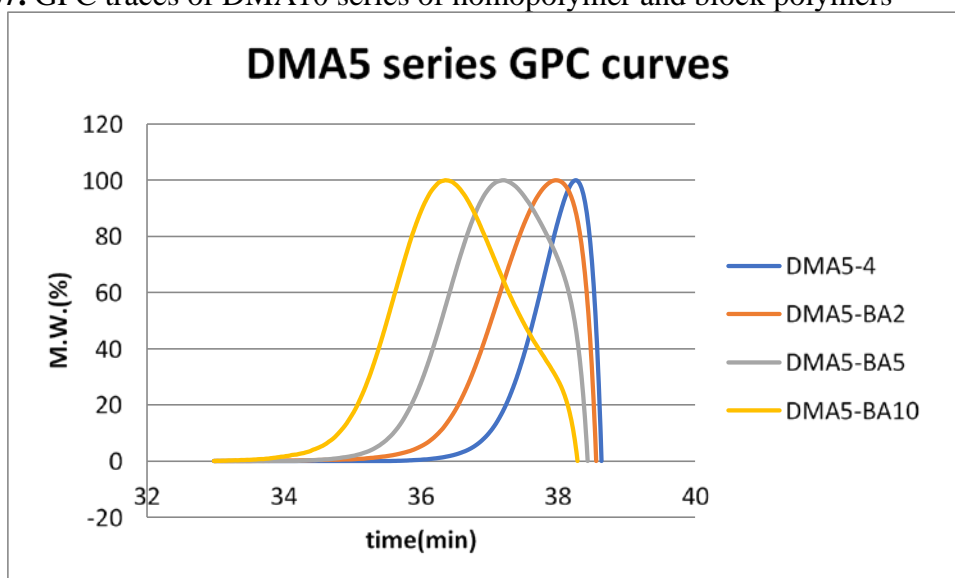


Figure S8. GPC traces of DMA5 series of homopolymer and block polymers

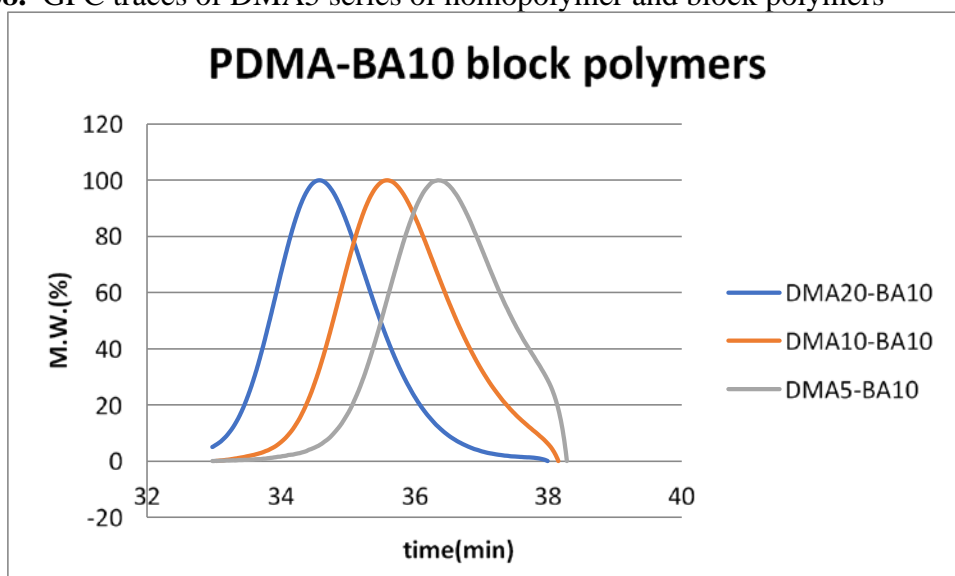


Figure S9. GPC traces of DMA n -BA10 series of block polymers

Part 2b. High Throughput “Surfactant-free” Emulsion Polymerization using PDMAM-block-PBA macroRAFT Agents

Materials

The PDMAM-block-PBA prepared in the experiments above were used directly. Styrene (Aldrich) was purified by passing through basic alumina immediately prior to use. The initiator, *p*-methane hydroperoxide (Lotus Chemicals, 53% active) was used as supplied. Sodium formaldehyde sulfoxylate (SFS, Bruggemann KG.). Iron (III) sulfate hydrate (Fe₂(SO₄)₃.xH₂O; Sigma Aldrich, 97 %). Diethanolamine (DHEA, Sigma-Aldrich, 98%).

Preparation of stock solutions

The polymerization mixtures A-I: comprising the components shown in Table S5 were prepared directly in the reactor vials. Only the mixtures comprising DMA20BA10 and DMA10BA10 were observed to give a stable dispersion of styrene monomer prior to polymerization.

Mixtures J and K comprising all components, except the additional styrene, were similarly prepared. The final 2 mL styrene was added by the robot after 2 hrs.

Stock solution L: styrene alone

Stock solution M: 0.5 g 2 wt% iron (III) sulfate hydrate solution + 0.5 g 10 wt% SFS solution + 9 g water.

Stock solution N: DHEA solution.(0.1 g DHEA in 9.9 g water)

All polymerization mixtures and stock solutions were degassed by nitrogen purging for 0.5 hour.

ChemSpeed Robotic Platform Synthesis.

The synthesis was conducted using a ChemSpeed[®] robotic synthesis platform which contained an iSynth reactor equipped with an array of 11 disposable glass reactor vials each with a capacity of 20 mL.

Stock solution M was injected into the 11 × 20 mL reactor vials containing solutions A-K and the reactor vials were vortexed at 400 rpm to commence polymerization. The polymerization was carried out at 20°C for 12 h with continued vortexing at 400 rpm..

For the polymerizations in reactors J and K were different from above. In these two reactors, a further 2 mL styrene was added after 2 h.

The polymerizations were carried out at 20 °C for a total time of 12 hrs. Polymerization was quenched by injection of DHEA solution (stock solution N).

Table S5. Composition of solutions for emulsion polymerization.

	Code	RAFT	RAFT g	KCl mg	Water mL	Styrene mL	Initiator ^b mL
A	DMA20BA2-St	DMA20BA2	0.2	30mg	9.8	2	0.2
B	DMA20BA5-St	DMA20BA5	0.2	30mg	9.8	2	0.2
C ^c	DMA20BA10-St	DMA20BA10	0.2	30mg	9.8	2	0.2
D	DMA10BA2-St	DMA10BA2	0.2	30mg	9.8	2	0.2
E	DMA10BA5-St	DMA10BA5	0.2	30mg	9.8	2	0.2
F ^c	DMA10BA10-St	DMA10BA10	0.2	30mg	9.8	2	0.2
G	DMA5BA2-St	DMA5BA2	0.2	30mg	9.8	2	0.2
H	DMA5BA5-St	DMA5BA5	0.2	30mg	9.8	2	0.2
I	DMA5BA10-St	DMA5BA10	0.2	30mg	9.8	2	0.2
J ^{c,d}	DMA10BA10-St2	DMA10BA10	0.2	30mg	9.8	0.2 + 2	0.2
K ^{c,d}	DMA20BA10-ST2	DMA20BA10	0.2	30mg	9.8	0.2 + 2	0.2

^a RAFT is PDMAm-*b*-PBA macroRAFT agent with code as indicated.

^b Initiator is *p*-menthane hydroperoxide.

^c Polymerization mixture appears to form stable emulsion before polymerization.

^d 0.2 g styrene added first, 2 g was added after 2 hours.

Characterization

Only four reactor vials (C, F, J and K) showed any sign of polymerisation having occurred and provided a stable latex. The other reactors showed immediate phase separation on being removed from the deck and there was no evidence of significant polymer precipitation or suspension being having been produced (Figure S10). The polymerization mixtures in reactors C, F, J and K were freeze-dried for analysis.

GPC analysis showed a bimodal distribution in each case (Figure S11). The M_p value of the longer retention time peak corresponded to the macroRAFT agent. If the contribution from the residual macroRAFT agent was subtracted, the dispersity of the polystyrene formed had low \bar{D} (< 1.2). GPC with UV detection showed the presence of the trithiocarbonate chromophore in the product proving that the product comprised residual macroRAFT agent rather than simply dead polymer.

Low monomer conversions in reactors C, F, J and K were attributed to the initiation system used but this was not further investigated. Subsequent work on batch RAFT emulsion polymerization of styrene made use of block macroRAFT agents DMA10BA10 and DMA20BA10 but used aqueous soluble initiators, e.g., potassium or ammonium persulfate in place of *p*-menthane hydroperoxide, and gave high monomer conversions.

Table S6. GPC analysis for styrene emulsion polymerizations.

Vial	MacroRAFT Code	Monomer	conversion (%)	M_n (GPC) ^a	M_p (GPC) ^{a,b}	\bar{D}
------	----------------	---------	----------------	--------------------------	----------------------------	-----------

F	DMA10BA10	styrene	<5	4103	8728	1.77
C	DMA20BA10	styrene	<5	12659	32147 5156	2.01
J	DMA10BA10-2	styrene	<5	3760	3335 8889	1.67
K	DMA20BA10-2	styrene	~15	11033	27794 4681	2.24

^a Polystyrene equivalents. ^b Peak molar mass.

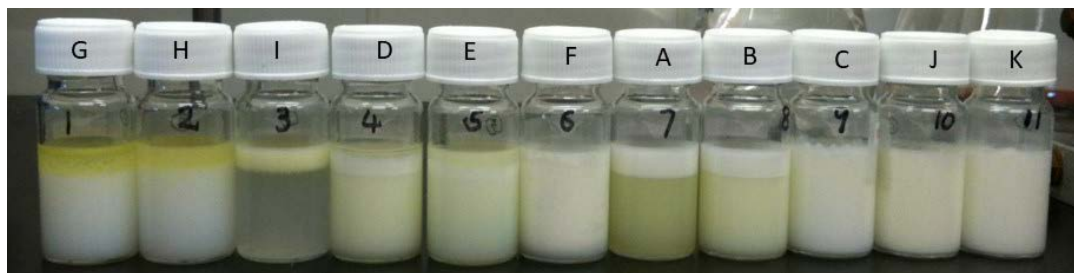


Figure S10. Reactor vials after polymerization. See Table S5 for vial designation.

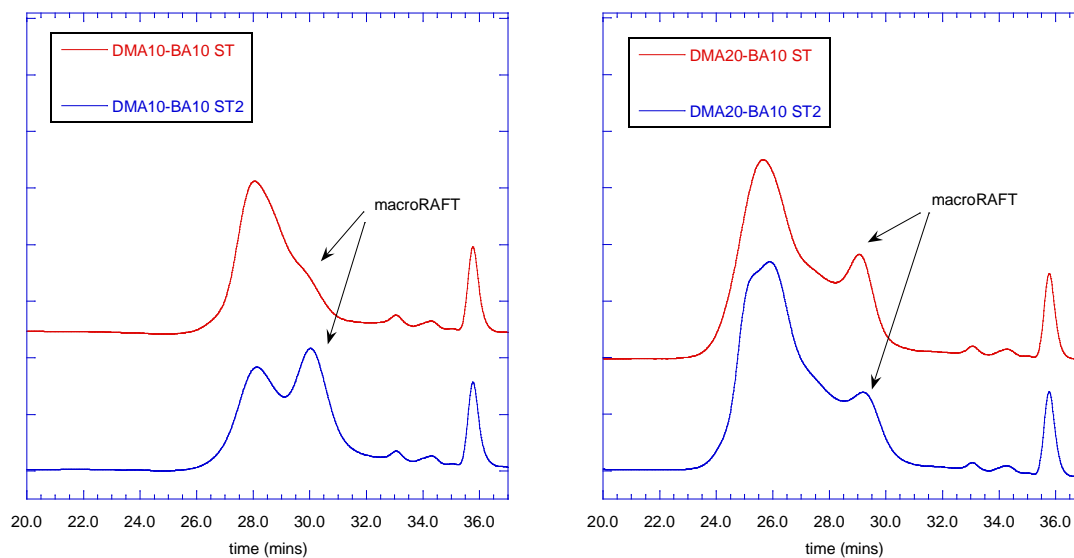


Figure S11. GPC traces for styrene emulsion polymers.

Part 3. Photo-RAFT Polymerization of liquid crystalline monomers

Materials

p-Hydroxybiphenyl (Sigma-Aldrich, 97%), methyl ethyl ketone (Sigma-Aldrich), triethylamine (Sigma-Aldrich, $\geq 99\%$), acryloyl chloride (Tokyo Chemical Industry, $> 98\%$), petroleum ether (Sigma-Aldrich, $\geq 90\%$ bp 40-60 °C), dichloromethane (Sigma-Aldrich, $\geq 99.8\%$), 4-cyano-4-(((dodecylthio)carbonothioyl)thio)pentanoic acid (BM1432, Boron Molecular, 97%), 2,2'-Azobis(2,4-dimethylvaleronitrile) (ABPN, Combi-Blocks, 95%), anisole (Sigma-Aldrich, 99%). All chemicals were used without further purifications.

Synthesis

4-biphenyl acrylate. The synthesis was adapted from the literature.^[2] *p*-Hydroxybiphenyl (10 g, 59 mmol) and butan-2-one (250 mL) were placed in a round-bottomed flask and triethylamine (8.2 mL, 59 mmol) was added. The mixture was cooled to 0 °C (ice bath) and acryloyl chloride (5.8 mL, 71 mmol) in butan-2-one (20 mL) was added dropwise at 0 °C. The mixture was left to stir for an extra 2 hours at 0 °C and then at room temperature (22 °C) overnight. The solution was filtered to remove the precipitated triethylamine salt and concentrated in vacuo. The crude product was purified by column chromatography using silica gel (pore size of 60 Å, high purity) eluting with 50:50 (v/v) petroleum ether (boiling range 60-80 °C):dichloromethane. A white powder (10.60 g, 80%) was obtained. m.p. 64.0-65.4 °C (lit.^[3] m.p. 64.5-65.0 °C); m/z (MH⁺ C₁₅H₁₂O₂H⁺ requires 225.09) found 225.0910; $\nu_{\max}/\text{cm}^{-1}$ 3036 (w, C=C-H, stretch), 1732 (s, C=O, stretch), 1638 (w, C=C, stretch), 1485 (m, C=C aromatic, bending), 1167 (s, C-O, stretching); δ_{H} (400 MHz, CDCl₃) 7.51-7.45 (4H, m, ArH), 7.34-7.30 (2H, m ArH), 7.26-7.21 (1H, m, ArH), 7.12-7.08 (2H, m, ArH) 6.52 (1H, dd, *J* 1.5, 17, H-C=C_{trans}), 6.23 (1H, dd, *J* 10, 17, H-C=C-C=O), 5.90 (1H, dd, *J* 1.5, 10, H-C=C_{cis}).

Poly(4-biphenyl acrylate) – Thermal-RAFT. The RAFT agent (4-cyano-4-(((dodecylthio)carbonothioyl)thio)pentanoic acid, 16 mg, 0.04 mmol) and the monomer (4-biphenyl acrylate, 897 mg, 4 mmol) were placed in a standard 4 mL vial and the initiator (2,2'-Azobis(2,4-dimethylvaleronitrile), 1.99 mg, 0.008 mmol) was then added from a stock solution (20 mg/mL in anisole, 202 mg). A further 1.4 g of anisole was added, the vial was closed with a Suba-Seal[®] septum and the solution was degassed by sparging with nitrogen for 15 minutes. The vial was thermostatted at 70 °C for 2 hours when the reaction was quenched by cooling down to room temperature and opened to air. The mixture was analysed by NMR spectroscopy and GPC. Monomer conversion = 92%, $M_{n,\text{GPC}} = 22,900$ g/mol, $D = 1.06$.

The polymerization of 4-biphenyl acrylate was conducted under essentially the same conditions in various solvents including those mentioned in Table S7. The GPC distribution for these are shown in Figure S12. Polymerization other than in anisole and DMF were observed to form a translucent, semi-opaque gel for conversions $> 15\%$. There was also significant dependence of the polymerization rate on solvent. Anisole appeared to provide the best combination of predicted M_n , low D , solution homogeneity and rapid polymerization rate.

Table S7. GPC analysis for dialkyldiazene-initiated RAFT polymerization at 70 °C in various solvents.

	Solvent	Conv. NMR (%)	$M_{n,th}$ (g/mol)	$M_{n,GPC}$ (g/mol)	\bar{D}
CB028-P1	DMF	97	21,400	18,100	1.19
CB028-P4	DMSO	97	21,700	23,300	1.09
CB028-P5	Anisole	97	20,000	18,100	1.08

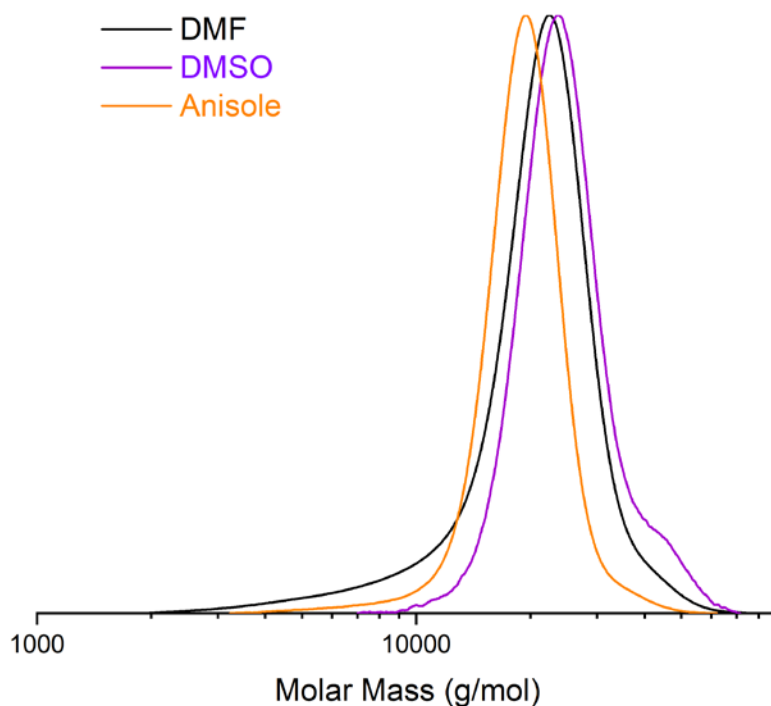


Figure S12. GPC molar mass distribution for ABPN-initiated RAFT polymerization at 70 °C in various solvents as indicated.

Poly(4-biphenyl acrylate) – Photo-RAFT. The following procedure is typical. A solution of the RAFT agent (4-cyano-4-(((dodecylthio)carbonothioyl)thio)pentanoic acid, 5.7 mg, 0.014 mmol), the monomer (4-biphenyl acrylate, 314 mg, 1.4 mmol), 328 mg of anisole and 77 mg of deuterated DMSO was prepared. The solution was transferred into a NMR tube and the solution was sparged with nitrogen for 15 minutes. The NMR tube was placed in a jacketed

holder in a photo-reactor operating at 451 nm (Figure S14).^[4] The light intensity, adjusted by means of a dimmer, was 13 W for all experiments. The jacket was thermostatted at 30 ± 2 °C. The reaction was stopped by turning off the light at near full monomer conversion as determined by ¹H NMR (i.e., 4 h) Monomer conversion = 90%, $M_{n,GPC} = 22,000$ g/mol, $D = 1.06$.

Details of the in-house constructed photoreactor and LED light source have been published previously.^[4] Measurements were conducted to estimate the average emission intensity for the 451 nm light source. The power output was measured in the middle of the LED reactor using a Powermax 5200 laser power meter. At a setting of 1.0 amp the measured electrical power was 12 W and the emission intensity was 8 W/m².

The GPC molar mass distributions for polymerization in conducted with various solvents are shown in Figure S13. Polymerizations with 90:10 anisole:DMSO or DMF remained as transparent yellow solutions, whereas polymerizations with DMSO or 50:50 anisole:DMSO as solvent were observed to form a translucent, semi-opaque gel for conversions > 15%. However, the polymerization in DMF was substantially slower with respect to the other systems with only 50% monomer conversion observed after 12 h irradiation. Gel formation in DMSO is attributed to self-assembly of the side chain liquid-crystalline polymer. Gel formation did not appear to limit control and there was no evidence of side reactions. The product was fully soluble for NMR and GPC analysis. It is possible gel formation reduces light penetration.

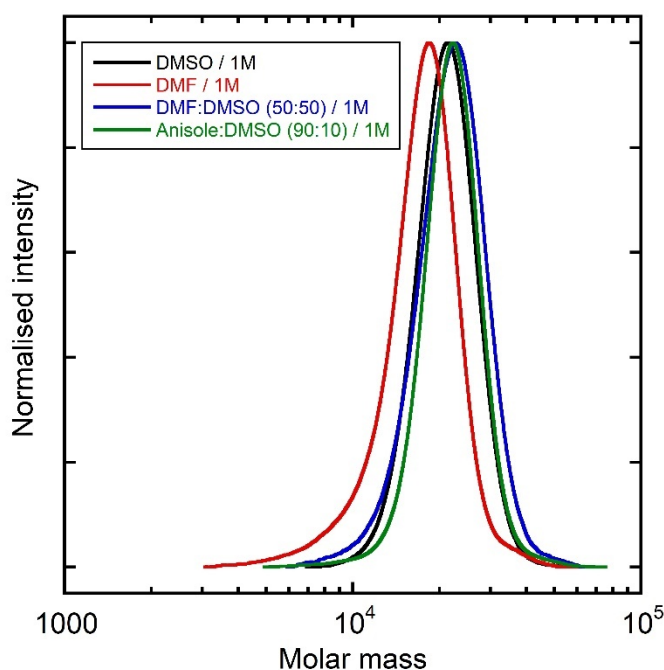


Figure S13. GPC molar mass distribution for polymerization in various solvents as indicated.



Figure S14. 451 nm photoreactor. Details have been published previously.^[4]

Characterization

Gel permeation chromatography (GPC) was performed on a Shimadzu system equipped with a CMB-20A controller system, an SIL-20A HT autosampler, an LC-20AT tandem pump system, a DGU-20A degasser unit, a CTO-20AC column oven, an RDI-10A refractive index detector, and 4 × Waters Styragel columns (HT2, HT3, HT4, and HT5, each 300 mm × 7.8 mm, providing an effective molar mass range of 100 – 4 × 10⁶ kDa). *N,N*-Dimethylacetamide (DMAc) (containing 4.34 g L⁻¹ lithium bromide (LiBr)) was used as an eluent with a flow rate of 1 mL/min at 80 °C. Number (M_n) and weight average (M_w) molar masses were evaluated using Shimadzu LC Solution software. The GPC columns were calibrated with low dispersity polystyrene (PSt) standards (Polymer Laboratories) ranging from 1,230 to 3,187,000 g/mol, and molar masses are reported as PSt equivalents. A 3rd-order polynomial was used to fit the log M_p vs time calibration curve, which was near linear across the molar mass range. All NMR spectra were recorded with a Bruker AV 400 MHz spectrometer at room temperature with either CDCl₃ or d-DMSO as solvent. Mass spectrometric analyses were performed on a Thermo Scientific Q Exactive mass spectrometer fitted with an ASAP ion source (M&M Mass Spec consulting). Positive and negative ions were recorded in an appropriate mass range at 140,000 mass resolution. The APCI probe was used without flow of solvent. The nitrogen nebulizing/desolvation gas used for vaporization was heated to 450 °C in these experiments. The sheath gas flow rate was set to 2, the auxiliary gas flow rate to 10 and the sweep gas flow rate to 2 (arbitrary units). The discharge current was 4 mA and the capillary temperature was 300 °C.

Determination of monomer conversion. Monomer conversion (p) was calculated from ¹H NMR data using the relative integration between an internal reference (anisole, CH₃ at 3.84 ppm) and the alkene region of the spectra (monomer, CH₂=CH-R at 5.5 – 6.6 ppm). The integration at the indicated time points was compared with that for zero time.

Calculation of the theoretical number-average molar mass ($M_{n,th}$). The theoretical number-average molar mass ($M_{n,th}$) was calculated using the following equation:

$$M_{n,th} = \frac{[M]_0 p M_M}{[RAFT]_0} + M_{RAFT}$$

where $[M]_0$ and $[RAFT]_0$ are the initial concentrations of monomer and RAFT agent, respectively; p is the monomer conversion as determined using Method 1; M_M and M_{RAFT} are the molar mass (g/mol) of the monomer and RAFT agent, respectively.

Part 4. Numerical Simulation of RAFT Polymerization Kinetics

The kinetic simulation of thermally initiated RAFT polymerization using PredecTM version 11 (CiT GMBH) was based on the reaction scheme shown in Scheme S1. This scheme has previously been used in modelling RAFT polymerization.^[5,6] In order to model direct RAFT photopolymerization we included the reactions shown in Scheme S2. The abbreviations for the major species are shown in Table S8.

There are a formidable number of rate coefficients associated with these reactions. It is nonetheless possible to assign reasonable values to these or show that the simulation is not sensitive to their precise values.

Initiation. The value of k_d is $2.46 \times 10^{-4} \text{ s}^{-1}$ for ABPN at $70 \text{ }^\circ\text{C}$ ^[7]. The initiator efficiency f is the initiator efficiency was assumed to be constant with monomer conversion and equal to 0.7.^[7] The value k_i for 2-cyano-4-methylpentan-2-yl radicals from ABPN and k_{iR} for 4-carboxy-2-cyanobutan-2-yl radicals from the initial RAFT agent adding to 4-biphenyl acrylate (BiA) were both taken to be the same as for 2-cyanoprop-2-yl radical adding to methyl acrylate,^[7,8] which we expect is a reasonable approximation. Thus, $k_i = k_{iR} = 1.18 \times 10^3 \text{ M}^{-1}\text{s}^{-1}$ at $70 \text{ }^\circ\text{C}$. The precise values of k_i and k_{iR} have little effect on the polymerization kinetics beyond the initialization period when the initial RAFT agent is converted to macroRAFT agent..

Propagation. Value of k_p for BiA have not been reported and the value might be assumed to be similar to k_p for phenyl acrylate. Azukizawa et al.^[9] have estimated a k_p for phenyl acrylate as $3580 \text{ M}^{-1}\text{s}^{-1}$ and k_t as $6.8 \times 10^6 \text{ M}^{-1}\text{s}^{-1}$ at $60 \text{ }^\circ\text{C}$ based on electron paramagnetic resonance spectroscopy measurements. This value is much lower than for other acrylates. However, we also note a strong solvent dependence on the rate of polymerization and the authors comment that their value might be affected by an unknown dependence on backbiting. Values of k_p for methyl, butyl and dodecyl acrylate in toluene at $70 \text{ }^\circ\text{C}$ are estimated to be 4.2, 4.0 and $3.5 \times 10^4 \text{ M}^{-1}\text{s}^{-1}$, respectively, based on the reported Arrhenius parameters,^[10] For the present study, the value of k_p was assumed to be $1.1 \times 10^4 \text{ M}^{-1}\text{s}^{-1}$ at $70 \text{ }^\circ\text{C}$. The precise value of k_p is not critical to the simulation except as it affects the values of the ratio k_p^2/k_t and the values of C_{tr} for the various RAFT agents and macroRAFT agents. The value of k_p also influences the length of the initialization period.

Termination. The value of k_t was then chosen as $2.0 \times 10^8 \text{ M}^{-1}\text{s}^{-1}$ at $70 \text{ }^\circ\text{C}$ independent of chain length, which gave the observed rate of polymerization. As in other radical polymerizations, the absolute values of k_p and k_t are not important in determining the polymerization rate, only the ratio k_p^2/k_t . Termination was assumed to be wholly by combination.^[11]

All primary radical termination with initiator or initial RAFT agent-derived radicals was taken to have a rate coefficient of $2.0 \times 10^9 \text{ M}^{-1}\text{s}^{-1}$.

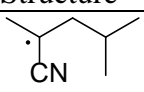
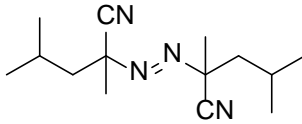
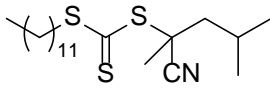
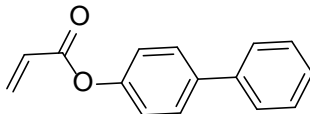
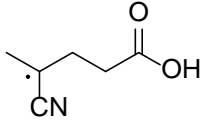
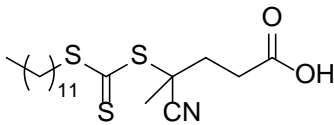
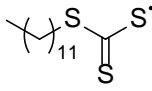
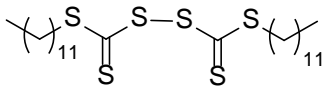
Addition-fragmentation chain transfer. The fragmentation rate coefficients for intermediates formed by addition to trithiocarbonates are known to be high and generally do not cause retardation. The values of all fragmentation rate coefficient were set to $1.0 \times 10^5 \text{ M}^{-1}\text{s}^{-1}$ at $70 \text{ }^\circ\text{C}$. Fragmentation of the intermediate derived from radicals adding to the initial RAFT agent is expected to be effectively irreversible in an acrylate polymerization with a tertiary cyanoalkyl RAFT agent. Note that as long as fragmentation is not rate determining, and in the absence of intermediate radical termination, only the values of k_{tr} and k_{-tr} are important in determining the molar mass distributions and the polymerization kinetics.^[12]

The rate of addition to the initial and macroRAFT agents were chosen to give the observed peak width at half height. The dispersities predicted by simulation are significantly larger than those measured experimentally due to the low sensitivity of RI for low molar mass chains (see text).

Intermediate radical termination was presumed not to occur. The process is not known to affect RAFT polymerization of acrylates with trithiocarbonates.

Photoinitiation. The additional reactions shown in Scheme 2 were included in order to model direct photo-initiated RAFT polymerization. Rate coefficients for unimolecular photodissociation of all RAFT agents and macroRAFT agents were assumed to be equal and the value was chosen so as to give the observed rate of polymerization. It is likely that the rate of photodissociation of the initial RAFT agent with a tertiary cyanoalkyl R group is higher than that of the poly(4-vinylbiphenyl) acrylate-based macroRAFT agent. In any event, the simulation is not sensitive to the precise value of the transfer coefficient of the initial RAFT agent. The rate coefficients for combination reactions involving the ZCS₂ radical were all assumed to be diffusion controlled and equal to that for primary radical termination ($2.0 \times 10^9 \text{ M}^{-1}\text{s}^{-1}$).

Table S8. Major species in simulation (Scheme S1 and Scheme S2)^a

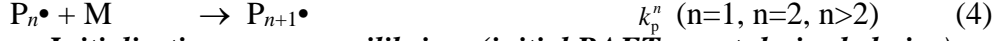
Abbreviation	Species	Structure
I•	initiator-derived radical	
I ₂	initiator	
I-I	product from self-reaction of initiator derived radicals	
I-Z	RAFT agent from initiator-derived radical	
M	monomer	
R•	radical derived from initial RAFT agent	
RZ	initial RAFT agent	
P _n •	propagating radical	
P _n Z	macro RAFT agent with chain length <i>n</i>	
P _{m+n} ^C	dead polymer formed by combination	
P _n ⁼	dead polymer formed by disproportionation with unsaturated end	
P _m ^H	dead polymer formed by disproportionation with saturated end	
Z•	thiocarbonylthio radical	
Z ₂	disulfide	

^a RAFT intermediates not shown.

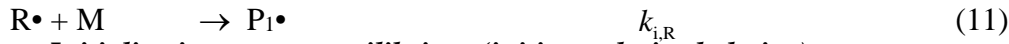
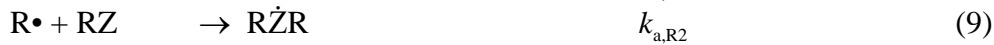
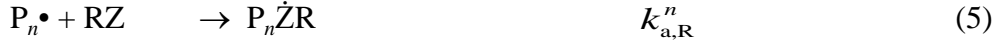
Initiation



Propagation



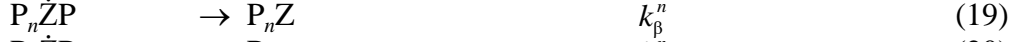
Initialization or pre-equilibrium (initial RAFT agent-derived chains)



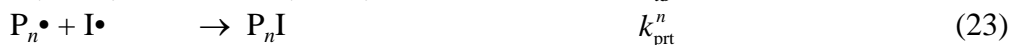
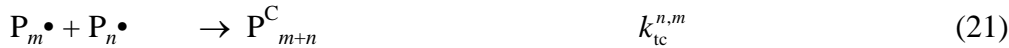
Initialization or pre-equilibrium (initiator-derived chains)



Main equilibrium

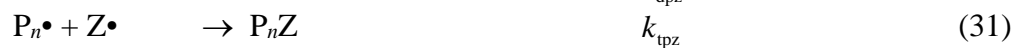


Termination



Scheme S1. Reaction scheme used in kinetic simulation of RAFT polymerization with a thermal initiator.

Photoinitiation (photoiniferter mechanism)



Scheme S2. Additional reaction used in kinetic simulation of direct RAFT photopolymerization.

References

- [1] Y.K. Chong, G. Moad, E. Rizzardo, S.H. Thang. *Macromolecules* **2007**, *40*, 4446-4455.
- [2] P.S. Vijayanand, S. Kato, M. Koyama, S. Satokawa, T. Kojima. *Designed Monomers and Polymers* **2007**, *10*, 375-388.
- [3] M. Baccaredda, P.L. Magagnini, G. Pizzirani, P. Giusti. *Journal of Polymer Science Part B: Polymer Letters* **1971**, *9*, 303-310.
- [4] A. Aerts, R.W. Lewis, Y. Zhou, N. Malic, G. Moad, A. Postma. *Macromol. Rapid. Commun.* **2018**, *39*, 1800240.
- [5] J.J. Haven, M. Hendrikx, T. Junkers, P.J. Leenaers, A. Postma, T. Tsompanoglou, C. Boyer, J. Xu, G. Moad, in *Reversible Deactivation Radical Polymerization: Mechanisms and Synthetic Methodologies* (Eds. K. Matyjaszewski; H. Gao; B.S. Sumerlin; N.V. Tsarevsky), **2018**, Vol. 1284, pp 77-103 (American Chemical Society: Washington, DC).
- [6] S. Houshyar, D. Keddie, G. Moad, R. Mulder, S. Saubern, J. Tsanaktsidis. *Polym. Chem.* **2012**, *3*, 1879-1889.
- [7] G. Moad. *Prog. Polym. Sci.* **2019**, *88*, 130-188.
- [8] H. Fischer, L. Radom. *Angew. Chem., Int. Ed. Engl.* **2001**, *40*, 1340-71.
- [9] M. Azukizawa, B. Yamada, D.J.T. Hill, P.J. Pomery. *Macromol. Chem. Phys.* **2000**, *201*, 774-781.
- [10] A.P. Haehnel, B. Wenn, K. Kockler, T. Bantle, A.M. Misske, F. Fleischhaker, T. Junkers, C. Barner-Kowollik. *Macromol. Rapid. Commun.* **2014**, *35*, 2029-2037.
- [11] T.G. Ribelli, K.F. Augustine, M. Fantin, P. Krysz, R. Poli, K. Matyjaszewski. *Macromolecules* **2017**, *50*, 7920-7929.
- [12] Y.K. Chong, J. Krstina, T.P.T. Le, G. Moad, A. Postma, E. Rizzardo, S.H. Thang. *Macromolecules* **2003**, *36*, 2256-2272.